Dalton Transactions

Accepted Manuscript

This article can be cited before page numbers have been issued, to do this please use: H. Imagawa, X. Wu, H. Itahara, S. Yin, K. Kojima, S. Chichibu and T. Sato, *Dalton Trans.*, 2018, DOI: 10.1039/C7DT04310D.

This is an Accepted Manuscript, which has been through the Royal Society of Chemistry peer review process and has been accepted for publication.

Accepted Manuscripts are published online shortly after acceptance, before technical editing, formatting and proof reading. Using this free service, authors can make their results available to the community, in citable form, before we publish the edited article. We will replace this Accepted Manuscript with the edited and formatted Advance Article as soon as it is available.

You can find more information about Accepted Manuscripts in the author guidelines.

Please note that technical editing may introduce minor changes to the text and/or graphics, which may alter content. The journal's standard Terms & Conditions and the ethical guidelines, outlined in our author and reviewer resource centre, still apply. In no event shall the Royal Society of Chemistry be held responsible for any errors or omissions in this Accepted Manuscript or any consequences arising from the use of any information it contains.

ROYAL SOCIETY OF CHEMISTRY

rsc.li/dalton

View Article Online
DOI: 10.1039/C7DT04310D

Journal Name

ARTICLE

Photocatalytic NO removal over calcium-bridged siloxenes under ultraviolet and visible light irradiation

Received 00th January 20xx,
Accepted 00th January 20xx

DOI: 10.1039/x0xx00000x

www.rsc.org/

Haruo Imagawa,[a]* Xiaoyong Wu,[b] Hiroshi Itahara,[a] Shu Yin,[b] Kazunobu Kojima,[b] Shigefusa F. Chichibu[b] and Tsugio Sato[b]

Ca-bridged siloxenes (Ca-siloxenes) composed of two-dimensional siloxene planes with Ca bridging were prepared and their photocatalytic properties for nitrogen oxide (NO) removal were investigated. Ca-siloxenes were synthesized via a solid-state metathesis reaction using $TaCl_5$ to extract Ca from $CaSi_2$ with different Cl_2/Ca molar ratios of 0.25, 1.25 and 2.5 (CS0.25, CS1.25 and CS2.5, respectively) in an attempt to control the amount of Ca extraction. Ca-siloxenes have a wide optical absorption band from the visible to ultraviolet region with absorption edges of 1.5, 2.9, 3.1 eV for CS0.25, CS1.25, and CS2.5, respectively. Ca-siloxenes exhibited photocatalytic activity for NO removal under irradiation with visible (λ > 400 nm (<3.10 eV)) and ultraviolet light (λ > 290 nm (<4.28 eV)). The photocatalytic activity was particularly improved by mixing the Ca-siloxene with acetylene black as a conductive material, which may have inhibited the recombination of photogenerated electrons and holes. The mixture of Ca-siloxene with acetylene black exhibited improved photocatalytic activity with the presence of $^1O_2$ as one of the active oxygen species formed under ultraviolet light irradiation.

1. Introduction

Nitrogen oxide (NOx) is known as an air pollutant that is mainly generated from combustion at industrial power plants and in automobiles. Several negative impacts of NOx on the environment have been recognized, such as the formation of acid rain, photochemical air pollution and ozone layer depletion. Therefore, trials to minimize the effects of NOx have been performed, and catalysts are often applied for NOx removal at the outlet of combustion systems. For example, selective catalytic reduction and lean NOx traps are useful devices for the removal of NOx in automobiles.[1-3] However, once released to the atmosphere, the removal of NOx is difficult under ambient conditions due to the low NOx concentration and energy sources required for the purification and regeneration of conventional catalysts.

Photocatalysts are one possible method to reduce NOx under ambient conditions with the use of sunlight irradiation as a natural resource. TiO_2 is the most common photocatalyst[4] and effective for photocatalytic NOx removal,[5] and other materials such as perovskite-type oxides have also been investigated.[6,7] Silicon-based materials have been investigated for hydrogen production by water splitting;[8-11] however, the application of Si-based materials to NOx removal is rare.[12]

In our previous study, we reported a novel calcium-bridged siloxene (Ca-siloxene) produced via a convenient solid-state metathesis reaction with an ethanol wash (Scheme 1).[13,14] In this synthesis, Ca is extracted from layered $CaSi_2$ with the help of $TaCl_5$ as a Cl source to form $CaCl_2$, while maintaining partial Ca-bridging between Kautsky-type siloxene planes[15,16] with Si_6 rings connected through Si-O-Si bridges. The presence of Kautsky-type siloxene planes was determined using Raman and Fourier transform-infrared spectroscopy measurements, which showed Si_6 rings in Si-based planes and those connected through Si-O-Si bridges, respectively.[13] Ca-bridging in Ca-siloxenes was characterized using X-ray absorption fine structure, which showed the presence of Si-Ca bonding.[13] The extent of Ca-extraction and the amount of resultant Ca-bridging are controlled by variation of the $TaCl_5$ concentration, and both primary and secondary particles become smaller with increased pore volumes as the Cl_2/Ca molar ratio is increased by fragmentation.[13,14]

Scheme 1 The solid state reaction employed for Ca-siloxene synthesis.

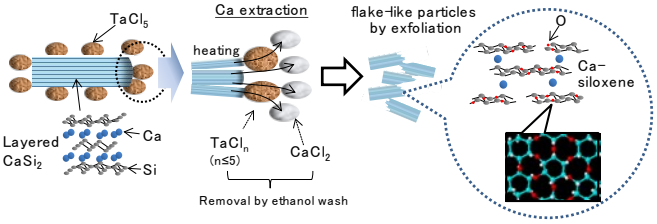

[a] Toyota Central R&D Labs., Inc. 41-1 Yokomichi, Nagakute, Aichi, 480-1192 Japan. e1152@mosk.tytlabs.co.jp
[b] Institute of Multidisciplinary Research for Advanced Materials, Tohoku University, 2-1-1 Katahira, Aoba-ku, Sendai 980-8577, Japan.

† Electronic Supplementary Information (ESI) available: X-ray diffraction data and *apparent quantum efficiency of* Ca-siloxenes. See DOI: 10.1039/x0xx00000x

Ca-siloxene had advantages over conventional Kautsky-type siloxenes. For example, the structural stability of Ca-siloxene based on its Ca-bridging was confirmed as responsible for its stable charge and discharge performance as a Li-ion battery anode.[14] Similar phenomenon for stability by ion intercalation has been also reported in 2D materials such as graphene and g-C_3N_4 for enhancing the interlayer van der Waals force[17,18] for photocatalysis.[19,20] In addition, it has been suggested that Ca-siloxene had a tunable direct bandgap energy that is dependent on the amount of Ca-bridging.[13]

A bare Ca-siloxene was reported to exhibit photocatalytic NO removal;[12] however, its compositional dependence was not examined. It was also implied that the addition of metallic particles may enhance the photocatalytic activity of the bare Ca-siloxene.[12] Herein, we report a systematic investigation of these points; the Ca-siloxenes are characterized with respect to optical and electrical properties by variation of the extent of Ca extraction in the synthesis step and the amount of conductive additives. The photocatalytic NO removal by Ca-siloxenes and the effect of conductive additives on the photocatalytic performance under ultraviolet and visible light irradiation are also discussed as a potential application. Chemiluminescence emission measurement for phosphorescence decay is also conducted to deduce a possible reactive species for photocatalytic NO removal.

2. Experimental

2-1. Synthesis of Ca-siloxenes[13]

Ca-siloxenes were synthesized using Cl_2/Ca molar ratios of 0.25, 0.5 and 2.5 (CS0.25, CS1.25 and CS2.5, respectively). In the synthesis, $CaSi_2$ (3.2, 1.6 and 0.32 mmol for CS0.25, CS1.25 and CS2.5, Rare Metallic Co.) and $TaCl_5$ (0.32 mmol, Wako Pure Chemical) were used as starting materials. A mixture of $CaSi_2$ and $TaCl_5$ were placed in boron nitride (BN) crucibles. These mixtures were calcined at 215 °C for 5 h at a heating rate of 100 °C h^{-1}. The mixtures packed in the BN crucibles were subsequently placed in sealed stainless steel cells (inner volume of 10 cm^3). The products were then washed with anhydrous ethanol to remove by-product $CaCl_2$ and excess $TaCl_5$ or their derivatives, before drying under vacuum at 80 °C. Each step in the synthesis was conducted under an Ar atmosphere. Kautsky-type siloxene as a reference sample was synthesized by the oxidation of $CaSi_2$ with HCl aqueous solution, as previously described in the literature,[15,16] and $CaSi_2$ was also used as a reference sample. To examine the effects of mixing conductive materials in the samples, Ca-siloxene/acetylene black (AB) mixtures with mass ratios of 99/1, 95/5, 90/10, and 70/30 were prepared.

2-2. Characterization of Ca-siloxenes

The crystalline structures of Ca-siloxenes were investigated using X-ray diffraction (XRD; Rigaku RINT-TTR). Ultraviolet (UV)/visible absorption spectra were acquired with a spectrometer (JASCO V-670) over a 2 mm diameter of each sample in the diffuse reflectance mode from 200 to 2500 nm at room temperature under air. Optical bandgap energy values were derived from Tauc plots[21] of the associated absorption data processed under the Kubelka-Munk function,[22] based on following equations (1)-(3):

$$F(R_\infty) = (1-R_\infty)^2/2R_\infty = K/S, \quad (1)$$

$$R_\infty = R_\infty(\text{sample})/R_\infty(\text{standard sample}), \quad (2)$$

$$(F(R_\infty)h\nu)^{1/n} = A(h\nu-E_g), \quad (3)$$

where R_∞ is the absolute reflectance, K is the absorption coefficient, S is the scattering coefficient, hν is the photon energy, n is determined according to the transition mode, A is a coefficient, and E_g is the optical bandgap or the absorption edge. $BaSO_4$ was used as a standard sample, and n = 1/2 was applied for direct allowed transitions, as suggested for Ca-siloxenes.[12,13]

The electrical conductivity of the samples was evaluated using the two-probe method with pelletized specimens at room temperature under air. These samples were uniaxially pressed at 8 MPa under DC current application.

Scanning electron microscopy (SEM) image of CS0.25 with 10 wt% of acetylene black was obtained for morphology characterization, using a Hitachi S-3600N.

2-3. Photocatalytic properties

The photocatalytic performance of the samples was measured based on the NO concentration at the outlet of the reactor using a NOx analyzer (Yanaco, ELC-88A) in the same manner as published in the literature.[7,12,23,24] The reactor volume was 373 cm^3 and the size of the sample glass holder was 20×15×0.5 mm. A constant flow rate of 200 mL min^{-1} of 1 ppm NO-50 vol% air with N_2 balance was applied for the reaction. Before light irradiation, the reactor with samples was purged under constant flow of the 1 ppm NO-50 vol% air with N_2 balance for 10 min to achieve diffusion and adsorption balance. Light was irradiated using a 450 W high-pressure mercury lamp using wavelengths of λ >290 nm (<4.28 eV) or >400 nm (<3.10 eV) with filtering out the UV emission. NO conversion was calculated based on the following equation (4):

$$\text{NO conversion (\%)} = 100 \times C_{NO}/C_{NO\text{-feed}} \quad (4)$$

where C_{NO} is the NO concentration measured by NOx analyzer at the outlet of the reactor and $C_{NO\text{-feed}}$ is the feed NO concentration measured before light irradiation. Durability tests were conducted by alternately switching UV light (λ > 290 nm (<4.28 eV)) on and off for 1 h each.

The apparent quantum efficiency was calculated based on the following equation (5):[24]

$$\Phi(\%) = 100 \times F_{NO}\alpha_\lambda/P_\lambda SA_\lambda, \quad (5)$$

where F_{NO} (μmol s^{-1}) is the NO amount rate in the feed gas, α_λ is NO conversion of samples (%), P_λ (μmol s^{-1}) is the light intensity on the surface of sample holder (λ >290 nm: 1139.8 (μmol s^{-1}), >400 nm: 846.7 (μmol s^{-1})), S is the surface area of sample holder(1.28 x 10^{-3} m^2), and A_λ is the average light absorption ratio of samples at different light wavelength based on UV/visible absorption spectra.

The phosphorescence decay profile of singlet oxygen ($^1O_2$) at a wavelength of 634 nm was measured after UV light (λ = 375 nm) irradiation for 5 s using a multiluminescence spectrometer (Tohoku Electric Ind., MLA-GOLDS). The data was obtained by subtracting the luminous intensity of λ > 640 nm from that of λ > 620 nm using two different cutoff filters.

3. Results and discussion

3-1. Characterization of Ca-siloxenes for optical and conductive properties

After the reaction of $CaSi_2$ with $TaCl_5$, synthesized samples exhibited broad peaks in the region from 25 to 40° due to the formation of an amorphous phase (Fig. S1). Although CS0.25 contained a crystalline phase derived from unreacted $CaSi_2$, broad peaks became dominant in CS1.25 and CS2.5, which suggests the fragmentation of layered $CaSi_2$ by Ca extraction and simultaneous exfoliation during synthesis.[13] Thus, CS0.25 is composed of a mixture of Ca-siloxene particles and remaining crystalline $CaSi_2$ particles, of which the average molar ratio of Ca and Si is Ca:Si = 0.61:2.[14] On the other hand, CS1.25 and CS2.5 are mainly composed of Ca-siloxene particles with average Ca:Si molar ratios of 0.27:2, and 0.09:2, respectively.[14]

UV/visible absorption spectra of Ca-siloxenes and Kautsky-type siloxene measured in the diffuse reflectance mode are shown in Fig. 1(A). Absorption spectra were measured from 200 nm (6.20 eV) to provide more accurate spectra in the UV region in contrast to those measured from 300 nm (4.13 eV) in our previous work.[13] All Ca-siloxenes had a characteristic broad absorption band ranging from the UV to visible light region with a clear peak at less than 250 nm and a shoulder and/or a peak at around 400 nm, which may be preferable for photocatalytic reactions from visible to ultraviolet light irradiation. All the Ca-siloxene samples exhibited semiconducting characteristics due to the Ca-extraction synthesis, in contrast to metallic $CaSi_2$. According to the Tauc plots produced with the assumption of direct transition (Fig. 1(B)), the absorption edges were increased with the Cl_2/Ca molar ratio during the synthesis step, and were determined to be 1.5, 2.9, and of 3.1 eV for CS0.25, CS1.25, and CS2.5, respectively. Siloxene has layered 2D Si-based planes composed of $Si_6O_3H_6$ with Si_6 rings connected through Si-O-Si bridges.[15,16] It has been reported that the siloxene structure exhibits direct optical transition due to the presence of oxygen (O) atoms in Si planes with σ-n mixing of Si σ electrons and O lone-pair electrons, unlike amorphous Si (a-Si) or polysilane structures.[25] The lowest unoccupied conduction band

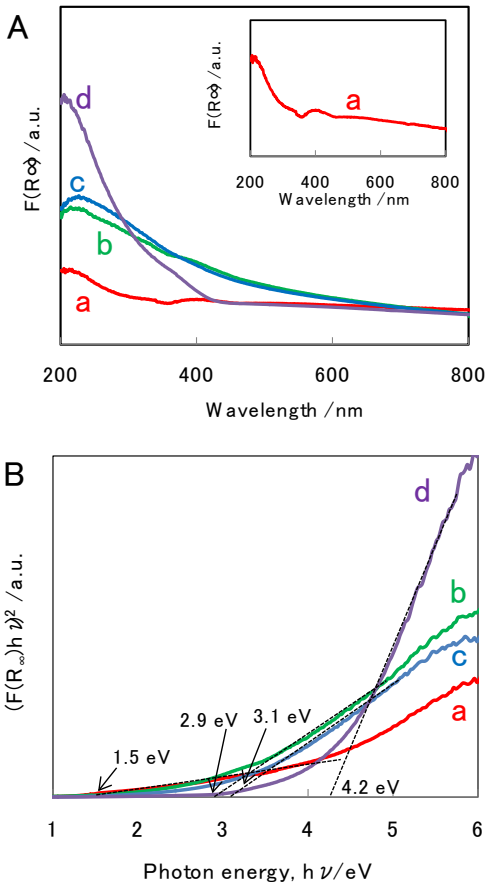

Fig. 1 (A) UV/visible spectra of Ca-siloxenes and (B) Tauc plots based on UV/visible spectral data; (a) CS0.25, (b) CS1.25, (c) CS2.5, and (d) Kautsky-type siloxene. Inset in (A): enlarged UV/visible spectra of CS0.25.

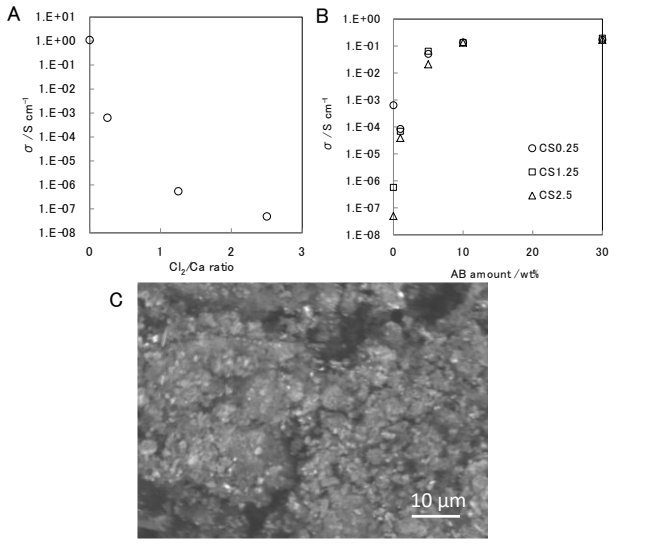

Fig. 2 Electrical conductivity of (A) Ca-siloxenes as a function of Cl_2/Ca ratio and (B) the mixture of Ca-siloxene and acetylene black (AB) as a function of AB amount, and (C) SEM image of CS0.25 with 10 wt% of AB.

View Article Online
DOI: 10.1039/C7DT04310D

composed of Si planes is reduced by the electron withdrawing property of O atoms, and the highest occupied valence band is formed by O lone-pair electrons, which leads to broadening of the bandgap. In the case of Ca-siloxenes, the amount of O atoms increased with the extent of Ca extraction according to Cl_2/Ca ratio during the synthesis step: $Ca_{1.8}Si_6O_{1.5}$ for CS0.25 and $Ca_{0.3}Si_6O_{2.8}$ for CS2.5.[13] Therefore, it would be possible to control the bandgap energy of the Ca-siloxene according to the amount of incorporated O atoms. The optical band gap energy of the Kautsky-type siloxene was determined as 4.2 eV, which was larger than those previously reported (2.5-2.9 eV) in the literature.[16,25] The measurements in the previous studies were typically conducted with light of less than 4.13 eV (300 nm) because those Si-based materials were considered to primarily absorb light below ca. 4 eV.[13] However, the previous study showed that similar Si-based materials could absorb light with higher photon energies of up to ca. 6 eV.[12] The density of states generally show a sharp increase at photon energies higher than that of the absorption edge; however, density of states with slight tailing at lower energy are often observed in the case of doped materials or impurity fluctuations. The adsorption edge is derived by extrapolation of the linear region of the Tauc plots observed at higher photon energy. Thus, photon energies of up to 6.20 eV (200 nm) were used for clarification in the present study, which corresponds to a widening of the measured energy by ca. 2 eV, and the impact at lower energy was reduced. The optical band gap energy observed in this study for Ca-siloxene and the Kautsky-type siloxene would be more accurate than those of previous studies. The UV/visible spectra of the Ca-siloxenes also contain broad tailing at less than ca. 4 eV, especially in CS1.25 and CS2.5, in contrast to the conventional Kautsky-type siloxene. One of the reasons for this Urbach tail feature may be due to the amorphous structure of Ca-siloxenes with inconsistent particle size and composition.[26]

Fig. 2(A) shows the electrical conductivity of Ca-siloxenes with Ca-extraction to various extents. The conductivity is almost inversely proportional to the extent of Ca-extraction in the Ca-siloxenes, and the conductivity of CS0.25 was 0.64 mS cm^{-1}, which was the highest electrical conductivity of all the Ca-siloxenes examined. The conductivities of CS1.25 and CS2.5 were ca. 0.5 and 0.05 μS cm^{-1}, respectively. Therefore, some conductive materials, such as metal particles[12] and carbon nanotubes,[27] may assist the construction of an electron pathway in the photocatalytic reaction that inhibits the recombination of photogenerated electrons and holes, and which improves catalytic activity.[12,27] The electrical conductivity of the mixture of Ca-siloxenes and AB as a conductive material is shown in Fig. 2(B). The conductivity was increased with the amount of AB additive and reached 0.1 S cm^{-1} at 10 wt% or more. Fig.2(C) shows the SEM image of CS0.25 with 10 wt% of AB. Almost consistent mixture of Ca-siloxene secondary particles with relatively larger size and AB secondary particles with less than 1μm diameter was observed, which reflect the increased conductivity shown above. Thus, 10 wt% of AB seems to be sufficient to cover almost all surfaces of the Ca-siloxene particles. The effect of the addition of conductive materials on the increased activity for NO removal is investigated in the next section.

3-2. Photocatalytic NO removal by Ca-siloxenes

Fig. 3(A) shows the NO conversion over Ca-siloxenes under UV light irradiation (λ > 290 nm (<4.28 eV)). Photocatalytic NO removal was observed with all the Ca-siloxene samples, and NO conversion was affected by the mixing AB with

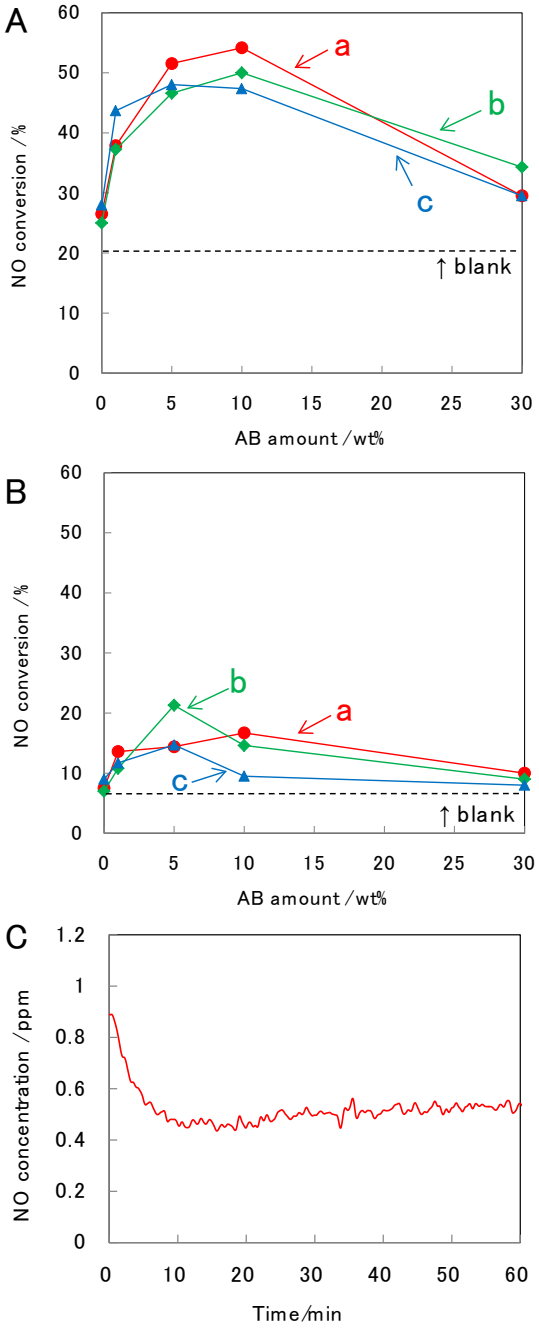

Fig. 3 NO conversions of Ca-siloxenes irradiated at (A) λ > 290 nm and (B) λ > 400 nm as a function of acetylene black amount:(a) CS0.25, (b) CS1.25 (c) CS2.5, and (C) NO conversion of CS0.25 with 10 wt% of acetylene black as a function of irradiation time at λ > 290 nm.

View Article Online
DOI: 10.1039/C7DT04310D

Ca-siloxenes in all the samples. The removal of NO is expected to form N_2 and HNO_3, as often reported with TiO_2 catalysts, with the aid of a small amount of water in air.[24,28,29]

NO conversion was increased with the amount of AB up to 10 wt%, and the maximum NO conversion was observed for the photocatalysts containing 10 wt% AB. This tendency corresponds to the electrical conductivity of the Ca-siloxene and AB mixtures. The low electrical conductivity of Ca-siloxene may cause the recombination of photogenerated electrons and holes, which results in low photocatalytic performance. As discussed in section 3-1, all Ca-siloxene particles were contacted with the addition of 10 wt% AB, and thereby reached the highest photocatalytic performance. On the other hand, NO conversion of all samples mixed with 30 wt% AB showed a drop in photocatalytic performance. AB itself has no photocatalytic activity and thus the decrease in the amount of Ca-siloxene in the samples corresponds to the decrease in NO conversion over the samples with 30 wt% AB. Best photocatalytic performance was observed in CS0.25 with 10 wt% AB addition. One reason of this performance was caused by the largest electric conductivity of CS0.25 in all Ca-siloxenes.

Fig. 3(B) shows the NO conversion of Ca-siloxenes under visible light irradiation (λ > 400 nm (<3.10 eV)). Samples mixed with 2.5-10 wt% AB exhibited clear photocatalytic activity for NO removal, although NO conversion under visible light irradiation was less than that under UV light irradiation. The absorption in the visible light region is present in all Ca-siloxenes, as shown in Fig. 1; however, the intensity was not as high relative to that observed in the UV light region, which resulted in the relatively lower photocatalytic activity.

To confirm the activity change, Fig. 3(C) demonstrates the NO conversion of CS0.25 with 10 wt% AB under UV light irradiation during 60 min. The photocatalytic activity was almost constant, and obvious decrease of activity was not observed, which supports the stability of Ca-siloxenes during photocatalytic reaction.

The apparent quantum efficiency of samples mixed with 10 wt % AB was roughly estimated in Fig. S2. The apparent quantum efficiency under UV light irradiation (λ > 290 nm) was around 0.0065 %, which is almost 1/4 of that found in TiO_2 species under the similar experimental condition using mercury lamp.[24] The apparent quantum efficiency under visible light irradiation (λ > 400 nm) was around 0.0017 % of CS2.5 to 0.0028 % of CS0.25.

For photocatalytic NO removal using TiO_2, oxygen radicals ($\cdot O_2$) are formed from O_2 at the conduction band and hydroxylradicals (·OH) are formed from H_2O at the valence band.[23] $^1O_2$ has also been known as one of the active oxygen species formed by the oxidation of $\cdot O_2$ through electron transfer at photogenerated holes during photocatalytic oxidation,[30] and $^1O_2$ is also known to have higher energy than ground-state triplet oxygen for the enhancement of photocatalytic NO removal.[28] $^1O_2$ is detectable from the typical dimol emissions around at 634 and 703 nm ($^1O_2 + {}^1O_2 \rightarrow 2{}^3O_2 + h\nu$), and from the monomol emission at 1270 nm ($^1O_2 \rightarrow {}^3O_2 + h\nu$).[28] Phosphorescence decay profile at 634 nm using a cut-off filter after UV light irradiation for 5 s were measured and are shown in Fig. 4. The Ca-siloxenes, especially CS0.25 and CS 2.5, exhibited phosphorescence decay derived from $^1O_2$ after UV light irradiation. The mixture of Ca-siloxenes and AB as a conductive additive may facilitate the oxidation of photogenerated $\cdot O_2$ to $^1O_2$ at available holes due to inhibition of the recombination of photogenerated electrons and holes, as reported for nanocomposite powders of Si nanoflakes and metallic particles.[12] Therefore, it is suggested that the same active oxygen species as proposed for photocatalysis with TiO_2 is also formed with Ca-siloxenes, which leads to N_2 and HNO_3 formation in the photocatalytic removal of NO.

3-3. Durability test

Durability tests of CS0.25 with 10 wt% of AB were conducted, and the results are shown in Fig. 5. Photocatalytic activity was almost maintained through the cycles, except for the initial deterioration during the first cycle. A rapid decrease in photocatalytic activity with degradation and deactivation through hydrogen release by hydrolysis has been reported for photocatalysis with siloxene in water.[31] In the present experiment, such deactivation and fading performance was not observed, although the Ca-siloxene was exposed to air

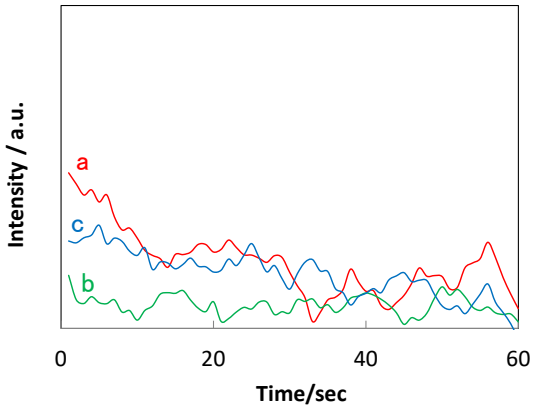

Fig. 4 Phosphorescence decay profile at 634 nm of $^1O_2$ generated at 298 K in air after 5 s UV light irradiation:(a) CS0.25, (b) CS1.25, and (c) CS2.5.

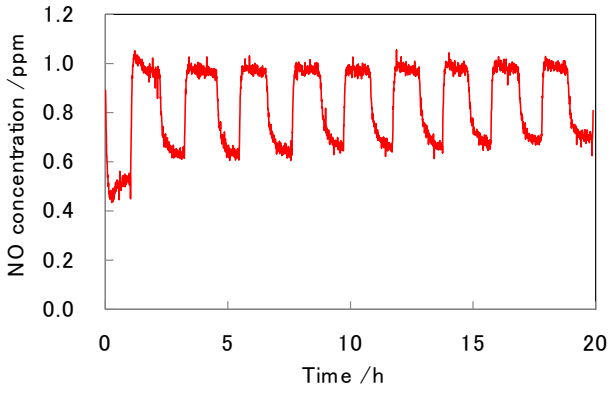

Fig. 5 NO concentration profiles of CS0.25 during durability test under the irradiation of ultraviolet light region (λ > 290 nm).

with a small amount of water during this photocatalytic reaction. Furthermore, siloxene has been reported to gradually form dangling bonds under ultraviolet light irradiation associated with structural degradation;[26] however, photocatalytic activity was almost maintained in the Ca-siloxenes, which implies structural stability due to the Ca-bridging of siloxenes. This is one for maintained photocatalytic activity in contrast to the siloxene structure with no bridges connecting the layered Si planes except for van der Waals forces, which allows unexpected cleavage between planes. The initial deterioration at the first cycle is explained as the adsorption of HNO_3 on the sample surface, which is formed as a product during NO removal reaction, which is known to lead to catalyst poisoning in TiO_2.[32,33] Therefore, the observed initial deterioration is considered to be similar poisoning, although the Ca-siloxenes are not influenced further by HNO_3 after the initial poisoning.

4. Conclusions

Ca-siloxenes with two-dimensional siloxene planes formed by Ca-bridging were synthesized, and their optical and electrical properties, and photocatalytic performance for NO removal were investigated. The Ca-siloxenes exhibited a wide and tunable optical absorption band from the visible to ultraviolet region with bandgap energies from 1.5 to 3.1 eV. All the Ca-siloxenes exhibited photocatalytic activity for NO removal under visible to ultraviolet light irradiation, which was enhanced by mixing the Ca-siloxene with AB as a conductive material, probably due to the inhibition of recombination of photogenerated electrons and holes. The phosphorescence decay profile of the Ca-siloxenes suggested the presence of $^1O_2$ as an active oxygen species that enhances photocatalytic NO removal.

Acknowledgements

The authors acknowledge Dr. Yoshiki Yamazaki of Tohoku University for conducting the diffuse reflectance spectroscopy measurements.

Notes and references

1 V.I. Pârvulescua, P. Grangeb, B. Delmon, *Catal. Today*, 1998, **46**, 233–316.
2 R. Burch, P. J. Millington, *Catal. Today,* 1995, **26**, 185-206.
3 H. Imagawa, T. Tanaka, N. Takahashi, S. Matsunaga, A. Suda, H. Shinjoh, *J. Catal.*, 2007, **251**, 315-320.
4 A. Fujishima and K. Honda, *Nature,* 1972, **238**, 37-38.
5 R. Asahi, T. Morikawa, T. Ohwaki, K. Aoki, and Y. Tage, *Science*, 2001, **293**, 269-271.
6 D. Wang, J. Ye, T. Kako, and T. Kimura *J. Phys. Chem. B,* 2006, **110**, 15824-15830.
7 H. Li, S. Yin, Y. Wang, T. Sekino, S. W. Lee, and T. Sato, *J. Catal.*, 2013, **297**, 65-69.
8 F. Dai, J. Zai, R. Yi, M. L. Gordin, H. Sohn, S. Chen and D. Wang, *Nature commun.*, 2014, **5**, doi:10.1038/ncomms4605.
9 T. Li, J. Li, Q. Zhang, E. Blazeby, C. Shang, H. Xu, X. Zhang and Y. Chao, *RSC Adv.*, 2016, **6**, 71092-71099.
10 Y. J. Jang, J. Ryu, D. Hong, S. Park and J. S. Lee, *Chem. Commun.*, 2016, **52**, 10221-10224.
11 J. Ryu, Y. J. Jang, S. Choi, H. J. Kang, H. Park, J. S. Lee and S. Park, *NPG Asia Materials*, 2016, **8**, e248.
12 H. Itahara, X. Wu, H. Imagawa, S. Yin, K. Kojima, S. F. Chichibu and T. Sato, *Dalton Trans.,* 2017, **46**, 8643-8648.
13 H. Imagawa, N. Takahashi, T. Nonaka, Y. Kato, K. Nishikawa and H. Itahara, *J. Mater. Chem. A*, 2015, **3**, 9411-9414.
14 H. Imagawa and H. Itahara, *Dalton Trans.,* 2017, **46**, 3655-3660.
15 H. Kautsky, W. Vogell, and F. Oeters, *Z. Naturforsch, B* 1955, **10**, 597-598.
16 S. Yamanaka, H. Matsu-ura, and M. Ishikawa, *Mater. Res. Bull.,* 1996, **31**, 307-316.
17 J. Abraham, K. S. Vasu, C. D. Williams, K. Gopinadhan, Y. Su, C. T. Cherian, J. Dix, E. Prestat, S. J. Haigh, I. V. Grigorieva, P. Carbone, A. K. Geim and R. R. Nair, *Nat. Nanotechnol.,* 2017, **12**, 546–550.
18 L. Chen, G. Shi, J. Shen, B. Peng, B. Zhang, Y. Wang, F. Bian, J. Wang, D. Li, Z. Qian, G. Xu, G. Liu, J. Zeng, L. Zhang, Y. Yang, G. Zhou, M. Wu, W. Jin, J. Li and H. Fang, *Nature,* 2017, DOI: 10.1038/nature24044.
19 J. Li, W. Cui, Y. Sun, Y. Chu, W. Cen and F. Dong, *J. Mater. Chem. A,* 2017, **5**, 9358-9364.
20 T. Xiong, W. Cen, Y. Zhang, and F. Dong, *ACS Catal.*, 2016, **6**, 2462-2472.
21 J. Tauc, R. Grigorovici and A. Vancu, *Phys. Status Solidi.*, 1966, **15**, 627.
22 P. Kubelka and F. Munk, *Zeit. Für Tekn. Physik*, 1931, **12**, 593.
23 S. Yin, B. Liu, P. Zhang, T. Morikawa, K. Yamanaka and T. Sato, *J. Phys. Chem. C*, 2008, **112**, 12425–12431.
24 H. Li, S. Yin, T. Sato, *Appl. Catal. B Environ.,* 2011, **106**, 586–591.
25 K. Takeda and K. Shiraishi, *Solid State Commun.,* 1993, **85**, 301-305.
26 H. Hirabayashi, K. Morigaki, and S. Yamanaka, *J. Phys. Soc. Jpn*., 1983, **52**, 671-676.1515
27 S. Takenaka, T. Arike, H. Matsune and M. Kishida, *Appl. Catal. B Environ.,* 2012, **125**, 358–366.
28 Y. Nosaka, T. Daimon, A. Y. Nosaka and Y. Murakami, *Phys. Chem. Chem. Phys.,* 2004, **6**, 2917–2918.
29 M. Anpo, In Recent DeVelopments on Visible Light Response Type Photocatalysts, NTS, Tokyo, 2002, p. 9.
30 T. Daimon, T. Hirakawa, M. Kitazawa, J. Suetake, and Y. Nosaka, *Appl. Catal. A General,* 2008, **340**, 169–175.
31 S. Li, H. Wang, D. Dandan Li, X. Zhang, Y. Wang, J. Xie, J. Wang, Y. Tian, W. Ni and Y. Yi Xie, *J. Mater. Chem. A*, 2016, **4**, 15841-15844.
32 Y. Ishibai, J. Sato, S. Akita, T. Nishikawa, and S. Miyagishi, *J. Photochem. Photobiol. A*, 2007, **177**, 106-111.
33 T. Ibusuki, and K. Takeuchi, *J. Mol. Catal*., 1994, **88**, 93–102.

Ca-bridged siloxenes with a wide optical absorption band from the visible to ultraviolet region exhibited photocatalytic activity for NO removal.